Radiation Modes and Step Discontinuities in Dielectric Rib Waveguide

Tullio Rozzi, *Fellow, IEEE,* Leonardo Zappelli, and M. N. Husain

Abstract—**Dielectric rib waveguides are common transmission lines in integrated optics, with interesting possibilities for millimetrics. Guided modes of uniform lines have been extensively investigated. In actual circuits, discontinuities or bends produce radiation from the waveguide, that can not be explained by means of the guided modes alone and inclusion of the continuous spectrum is essential in understanding the physical effects that arise there. In this work, we introduce the continuum of the rib waveguide, a part of the spectrum that was not reported up to date. The theory is applied to the abrupt step discontinuity in the E-plane of the rib guide under LSE polarization and to the abrupt termination problem, including radiative effects never investigated before.**

Introduction

THE STATE of the art in millimetric and integrated optical technology is such that fairly sophisticated circuits containing a number of components to perform complex functions are now realizable.

Rib waveguide is, possibly, the most widely used transmission medium in this connection, which has motivated a considerable modelling effort to characterize its guided modes (see [1]–[3], to mention just a few).

Realistic components, however, imply the presence of discontinuities, whose effect is not only to alter the propagation characteristics of the fundamental mode, but moreover to excite radiative and reactive unbound fields in the substrate and air regions.

Radiative fields can travel a long way in both regions and cause interaction with other components sharing the same substrate or cladding, particularly, in multilevel, multiple guide configurations.

It is therefore important at this time to ascertain what these fields are in rib guide.

The complete spectrum of multilayer slab waveguides is now well known. It consists of a few bound modes, if any, and a continuum of radiative and reactive air and substrate modes. The latter are real fields, finite at infinity, that under appropriate orthonormalization constitute, together with the bound modes, a complete description of any physical field around the guide, for instance, in presence of discontinuities, in a manner conceptually analogous to a modal expansion in a close guide.

This kind of information is, to date, not available for rib guide. Previous works on the step discontinuity either consider just the fundamental mode, which is fair enough in absence of serious radiative effects, or approach the problem by means of sophisticated numerical methods, such as Finite Elements [4]. Finite Elements, Beam Propagation Method or Method of Lines are used to investigate other kinds of discontinuities such as bends or Y-junction. For example, in [5] the curvature was examinated by means of the EDC transformation of the rib waveguide in a slab waveguide, and then applying the concept of the "local modes" to the study of the bend, taking into account the complete spectrum of the slab waveguide. In [6] and [7] the Method of Lines is used to characterize the curvature. In [8] the discontinuity of the Y-junction, made of rib waveguide, is also investigated by means of a new Explicit Finite Difference Beam Propagation Method (EFD-BPM).

Thus, while useful results are produced by numerical methods for isolated discontinuities, the presence of multiple discontinuities causes occupation of memory and computer time to grow with the cube of the dimensions of the structure.

Moreover, with a view to interpreting results and deriving simplified models, it is important to avail analytical tools that can be applied to this class of problems.

The analytical development is complicated by the nonseparable nature of the rib guide cross-section, involving diffraction transverse to x (see Fig. 1). Considerable progress, however, has been made since the first approach originally presented in [9] that treats in terms of 'partial waves' the germane problem of the continuum of image line. This new insight specialized to the case of the rib guide will be the object of the first half of this paper.

It introduces the concept of 'wave packets' that are individual solutions of the transverse diffraction problem satisfying boundary, edge and radiation conditions. Each packet is, in general, labelled by two indices, namely, the continuous transverse wavenumber k_t, and a discrete one, ν, identifying possible degenerate solutions pertaining to the same value of k_t. Each packet is fully characterized by a single 'phase shift' $\alpha_\nu(k_t)$, that is found by solving

Manuscript received August 2, 1991; revised March 30, 1992.

T. Rozzi and L. Zappelli are with the Dipartimento di Elettronica ed Automatica, Università di Ancona, Via Brecce Bianche, 60131, Ancona, Italy

M. N. Husain is with the School of Electrical Engineering, University of Bath, Bath, UK.

IEEE Log Number 9202130.

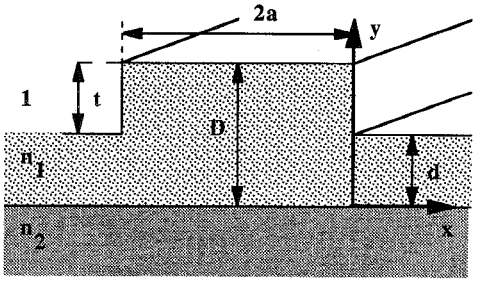

Fig. 1. The cross-section of the infinite rib waveguide.

an eigenvalue equation arising from field continuity at the discontinuous interface of the transverse step.

'Wave packets' (continuous modes) are amenable to orthonormalization and, together with the bound modes, constitute a complete spectrum of modes for the rib guide.

It is remarked that the full hybrid nature of the field in rib guide is not yet dealt with in the present contribution. This plays a significant role close to modal cutoff of the fundamental mode [10]–[13] and in those situations where the discontinuity may cause considerable cross-polarization [12]. Where the rib aspect ratio (t/2a) is sufficiently low, typically ≤ 0.4, the minor hybrid content of the field does not seem to warrant the additional complication involved. In the following, LSE polarization is assumed, but this assumption is removable if required.

In the second half of the paper, knowledge of the complete spectrum is applied to the practically important problem of two-dimensional steps in the guide.

Both here and in determining the spectrum, use is made of the concept of 'transition function', previously introduced in [3] in order to generate accurate first order variational solutions for the bound modes that considerably reduce the computational load.

Numerical results are presented for the reflection coefficient of a step in rib width and for three different abrupt terminations, that is, the abrupt termination of the rib, of the rib and guiding layer and of the whole guide. In the last case, the forward and backscattered radiated field is also evaluated.

Theory

Continuous Spectrum of the Infinite Rib Guide

As two indices are needed in order to represent the complete spectrum of a close bidimensional waveguide, two indices are also needed in this open problem.

Moreover, the complete spectrum must reproduce the whole range of the β-value on the complex plane: the real values correspond to radiating waves, the imaginary values to reactive effects. We use a continuous variable that labels the continuous spectrum, namely k_t, $k_t = (k_0^2 - \beta^2)^{1/2}$, with $0 \leq k_t \leq \infty$, (air continuous modes) or $\sigma_t = (k_0^2\epsilon_2 - \beta^2)^{1/2}$, with $0 \leq \sigma_t \leq v = k_0\sqrt{\epsilon_2 - 1}$ (substrate continuous modes). The whole continuous spectrum is therefore constituted by a propagating part ($k_t \leq k_0$ corresponding to $0 \leq \beta(k_t) \leq k_0$ and $0 \leq \sigma_t \leq v$ corresponding to $k_0 < \beta(\sigma_t) \leq k_0\sqrt{\epsilon_2}$), and a non-propagating one ($k_t > k_0$ corresponding to $\mathrm{Im}\{\beta(k_t)\} > 0$).

To a given k_t-value (or σ_t-value) may further correspond more than one field distribution, each satisfying the boundary conditions, that will be labelled by the discrete index ν. Hence, the unbound part of a typical field component, say H_y, can be written in terms of this spectrum as

$$H_y(x, y) = \int_0^{\infty} \sum_{\nu=1,2,\cdots} A_\nu(k_t)\, H_{y\nu}(x, y, k_t)\, dk_t + \int_0^{v} \sum_{\nu=1,2,\cdots} B_\nu(\sigma_t)\, H_{y\nu}(x, y, \sigma_t)\, d\sigma_t. \quad (1)$$

Each component of the continuous ('wave packet') is therefore completely labeled by two indices, the continuous index k_t (or σ_t) and the discrete index ν.

Transverse Step Discontinuity at $x = 0$

Finding the continuous spectrum of the rib waveguide, shown in Fig. 1, starts from the knowledge of the complete spectra of the two slabs constituting the structure. They include the surface waves, $\phi_s(y)$ for $x < 0$, $\psi_s(y)$ for $x > 0$, and the continua of the air regions $\phi_e(\rho, y)$, $\phi_0(\rho, y)$, $\psi_e(\rho, y)$, $\psi_o(\rho, y)$, e = even, o = odd and of the substrate regions $\phi_{sb}(\sigma, y)$, $\psi_{sb}(\sigma, y)$.

Considering transverse propagation in the x-direction, the presence of the discontinuity at $x = 0$ produces scattering among the slab modes. As in a discontinuity problem, a combination of these modes is required in order to satisfy all boundary and edge conditions imposed by the rib corner. Starting from these physical considerations, we suppose that there is only one surface wave in both slabs and electric wall symmetry at the rib plane of symmetry $x = -a$; we fix a given value of k_t and of the discrete index ν. We then choose a y-directed potential that is constituted by the superposition of slab modes of the following form (suppressing the factor $e^{-j\beta z}$)

$$\Pi_\nu^h(x, y, k_t) = \frac{P_\nu^-}{k_0^2\epsilon_{e-}}\phi_s(y)\frac{\cos[q_s(k_t)(x + a)]}{\cos[q_s(k_t)a]} + \sum_{m=e,o}\int_0^{\infty}\frac{Q_{\nu m}^-(\rho)}{k_0^2 - \rho^2}\phi_m(\rho, y) \cdot \frac{\cos[q(\rho, k_t)(x + a)]}{\cos[q(\rho, k_t)a]}\, d\rho + \int_0^{v}\frac{S_\nu^-(\sigma)}{k_0^2\epsilon_2 - \sigma^2}\phi_{sb}(\sigma, y) \cdot \frac{\cos[p(\sigma, k_t)(x + a)]}{\cos[p(\sigma, k_t)a]}\, d\sigma \quad -a \leq x \leq 0 \quad (2a)$$

$$\Pi_\nu^h(x, y, k_t) = \frac{P_\nu^+}{k_0^2\epsilon_{e+}} \psi_s(y) \frac{\cos[k_x(k_t)x + \alpha_\nu(k_t)]}{\cos \alpha_\nu(k_t)} + \sum_{m=e,o} \int_0^{k_t} \frac{Q_{\nu m}^+(\rho)}{k_0^2 - \rho^2} \psi_m(\rho, y) \cdot \frac{\cos[q(\rho, k_t)x + \alpha_\nu(k_t)]}{\cos \alpha_\nu(k_t)} d\rho + \sum_{m=e,o} \int_{k_t}^{\infty} \frac{Q_{\nu m}^+(\rho)}{k_0^2 - \rho^2} \psi_m(\rho, y) \cdot e^{-\gamma(\rho, k_t)x} d\rho + \int_0^{v} \frac{S_\nu^+(\sigma)}{k_0^2\epsilon_2 - \sigma^2} \psi_{sb}(\sigma, y) \cdot \frac{\cos[p(\sigma, k_t)x + \alpha_\nu(k_t)]}{\cos \alpha_\nu(k_t)} d\sigma \Bigg\} \quad x \geq 0 \tag{2b}$$

where e, o denotes parity of the continua of the slabs and, moreover:

$$k_x(k_t) = \sqrt{k_t^2 + k_0^2(\epsilon_{e+} - 1)}$$

$$q_s(k_t) = \sqrt{k_t^2 + k_0^2(\epsilon_{e-} - 1)}$$

$$p(\sigma, k_t) = \sqrt{k_t^2 - \sigma^2 + v^2} \qquad q(\rho, k_t) = \sqrt{k_t^2 - \rho^2}$$

$$\gamma(\rho, k_t) = \sqrt{\rho^2 - k_t^2} \qquad v = k_0\sqrt{\epsilon_2 - 1}$$

P_ν^-, P_ν^+, $Q_{\nu m}^-$, $Q_{\nu m}^+$, S_ν^-, S_ν^+ are as yet unknown amplitudes and ϵ_{e-}, ϵ_{e+} the effective dielectric constants of the slabs for $x < 0$, $x > 0$ respectively.

The form of (2a), (2b) requires some comment.

The x-dependence in (2a) arises from the even plane of symmetry at $x = a$, that in (2b) implies a standing wave in the external region. The latter can be seen as the combination of a wave $e^{jk_x x}$ generated by a source at $x = +\infty$ and travelling towards the discontinuity and a reflected wave $e^{-j(k_x x + 2\alpha_\nu(k_t))}$. The phase shift $\alpha_\nu(k_t)$ is of special significance.

It is noted that it is taken as a function of just $k_t = \sqrt{k_x^2 + k_y^2}$ and not of k_x, k_y separately.

This is an essential requirement in order that fields transverse to x derived from the same potential (2a), (2b) and travelling with the same phase velocity in the z-direction be continuous at the transverse step discontinuity, that is, they form a 'wave packet' individually satisfying the boundary conditions. In fact, taking into account that the fields in the LSE case are given by

$$E_{x\nu}(x, y, k_t) = \omega\mu\beta(k_t)\, \Pi_\nu^h(x, y, k_t)$$

$$E_{y\nu}(x, y, k_t) = 0$$

$$E_{z\nu}(x, y, k_t) = -j\omega\mu\partial_x \Pi_\nu^h(x, y, k_t)$$

$$H_{x\nu}(x, y, k_t) = \partial_{xy}^2 \Pi_\nu^h(x, y, k_t)$$

$$H_{y\nu}(x, y, k_t) = (k_0^2\epsilon_r + \partial_y^2)\, \Pi_\nu^h(x, y, k_t)$$

$$H_{z\nu}(x, y, k_t) = -j\beta(k_t)\, \partial_y \Pi_\nu^h(x, y, k_t)$$

we apply the continuity of the $H_{y\nu}(x, y, k_t)$ component at the interface $x = 0$. Denoting the interface field $H_{y\nu}(0, y, k_t) \equiv h_{y\nu}(y, k_t)$, we recover, from orthogonality of the slab mode functions, the following expressions for the amplitude coefficients P, Q, S at either side of $x = 0$:

$$P_\nu^- = \int_{-\infty}^{\infty} h_{y\nu}(y, k_t)\, \phi_s(y)\, dy \equiv \langle h_{y\nu}(y, k_t), \phi_s(y) \rangle$$

$$P_\nu^+ = \langle h_{y\nu}(y, k_t), \psi_s(y) \rangle$$

$$Q_{\nu m}^-(\rho) = \langle h_{y\nu}(y, k_t), \phi_m(\rho, y) \rangle$$

$$Q_{\nu m}^+(\rho) = \langle h_{y\nu}(y, k_t), \psi_m(\rho, y) \rangle$$

$$S_\nu^-(\sigma) = \langle h_{y\nu}(y, k_t), \phi_{sb}(\sigma, y) \rangle$$

$$S_\nu^+(\sigma) = \langle h_{y\nu}(y, k_t), \psi_{sb}(\sigma, y) \rangle$$

The analytical expressions of these coefficients are reported in [3].

As these coefficients are now expressed in terms of $h_{y\nu}$, we apply the continuity of $E_{z\nu}(x, y, k_t)$ at $x = 0$. From this equation, we obtain an eigenvalue equation for the as yet undetermined phase shift $\alpha_\nu(k_t)$, that is, the last unknown quantity in the expression (2a), (2b) for the potential. This is:

$$tg\alpha_\nu(k_t) \Bigg\{ \frac{P_\nu^+}{k_0^2\epsilon_{e+}} \psi_s(y)\, k_x(k_t) + \sum_{m=e,o} \int_0^{k_t} \frac{Q_{\nu m}^+(\rho)}{k_0^2 - \rho^2} \psi_m(\rho, y)\, q(\rho, k_t)\, d\rho + \int_0^{v} \frac{S_\nu^+(\sigma)}{k_0^2\epsilon_2 - \sigma^2} \psi_{sb}(\sigma, y)\, p(\sigma, k_t)\, d\sigma \Bigg\}$$

$$= -\sum_{m=e,o} \int_{k_t}^{\infty} \frac{Q_{\nu m}^+(\rho)}{k_0^2 - \rho^2} \psi_m(\rho, y)\, \gamma(\rho, k_t)\, d\rho + \frac{P_\nu^-}{k_0^2\epsilon_{e-}} \phi_s(y)\, q_s(k_t)\, tg[q_s(k_t)a] + \sum_{m=e,o} \int_0^{\infty} \frac{Q_{\nu m}^-(\rho)}{k_0^2 - \rho^2} \phi_m(\rho, y)\, q(\rho, k_t) \cdot tg[q(\rho, k_t)a]\, d\rho + \int_0^{v} \frac{S_\nu^-(\sigma)}{k_0^2\epsilon_2 - \sigma^2} \cdot \phi_{sb}(\sigma, y)\, p(\sigma, k_t)\, tg[p(\sigma, k_t)a]\, d\sigma. \tag{3}$$

On inspection and bearing in mind the definition of P, Q, S, (3) can be written more compactly as the following operator eigenvalue equation:

$$tg\alpha_\nu(k_t)\, \mathrm{Re}\{\tilde{Z}(k_t)\} \cdot h_{y\nu}(y, k_t) = \mathrm{Im}\{\tilde{Z}(k_t)\} \cdot h_{y\nu}(y, k_t) \tag{4}$$

where $\tilde{Z}(k_t) = \mathrm{Re}\{\tilde{Z}(k_t)\} - j\, \mathrm{Im}\{\tilde{Z}(k_t)\}$ is the transverse impedance integral operator acting on the field $h_{y\nu}(y,$

k_t) whose kernel $Z(y, y', k_t)$ is defined below:

$$\begin{aligned}\text{Re}\ \{Z(y, y', k_t)\} &= \omega\mu\Bigg\{\frac{k_x(k_t)}{k_0^2\epsilon_{e+}}\psi_s(y)\,\psi_s(y') \\ &+ \sum_{m=e,o}\int_0^{k_t}\frac{q(\rho, k_t)}{k_0^2-\rho^2}\psi_m(\rho, y)\,\psi_m(\rho, y')\,d\rho \\ &+ \int_0^{v}\frac{p(\sigma, k_t)}{k_0^2\epsilon_2-\sigma^2}\psi_{sb}(\sigma, y)\,\psi_{sb}(\sigma, y')\,d\sigma\Bigg\}\end{aligned}$$

$$\begin{aligned}\text{Im}\ \{Z(y, y', k_t)\} &= \omega\mu\Bigg\{-\sum_{m=e,o}\int_{k_t}^{\infty}\frac{\gamma(\rho, k_t)}{k_0^2-\rho^2}\psi_m(\sigma, y)\,\psi_m(\sigma, y')\,d\rho \\ &+ \frac{q_s(k_t)}{k_0^2\epsilon_{e-}}\phi_s(y)\,\phi_s(y')\,tg[q_s(k_t)a] \\ &+ \sum_{m=e,o}\int_0^{\infty}\frac{q(\rho, k_t)}{k_0^2-\rho^2}\phi_m(\rho, y)\,\phi_m(\rho, y') \\ &\cdot tg[q(\rho, k_t)a]\,d\rho + \int_0^{v}\frac{p(\sigma, k_t)}{k_0^2\epsilon_2-\sigma^2}\phi_{sb}(\sigma, y) \\ &\cdot \phi_{sb}(\sigma, y')\,tg[p(\sigma, k_t)a]\,d\sigma\Bigg\}.\end{aligned}$$

We may cast (4) in a variational form, by multiplying by $h_{yv}(y, k_t)$, integrating in y and obtaining:

$$tg\alpha_v(k_t) = \frac{\langle h_{yv}(y, k_t),\ \text{Im}\ \{\tilde{Z}(k_t)\},\ h_{yv}(y', k_t)\rangle}{\langle h_{yv}(y, k_t),\ \text{Re}\ \{\tilde{Z}(k_t)\},\ h_{yv}(y', k_t)\rangle}.$$

The above problem is amenable to a standard Ritz–Galerkin approach. Thus, we choose an appropriate orthonormal basis $\{f_k(y)\}$ in order to expand $h_{yv}(y, k_t)$:

$$h_{yv}(y, k_t) = \sum_{k=1}^{N} H_{kv} f_k(y). \tag{5}$$

Substituting (5) in (4) turns the latter integral equation into the following standard matrix eigenvalue problem:

$$\begin{aligned}tg\alpha_v(k_t)\ \text{Re}\ \{\mathbf{Z}(k_t)\}_{N\times N}[\boldsymbol{H}_v]_{N\times 1} \\ = \text{Im}\ \{\mathbf{Z}(k_t)\}_{N\times N}[\boldsymbol{H}_v]_{N\times 1}\end{aligned} \tag{6}$$

where $\mathbf{Z}(k_t) = \text{Re}\ \{\mathbf{Z}(k_t)\} - j\ \text{Im}\ \{\mathbf{Z}(k_t)\}$ is the transverse impedance matrix of the rib guide, defined elementwise by

$$\begin{aligned}\text{Re}\ \{\mathbf{Z}(k_t)\}_{ik} &= \frac{k_x(k_t)}{k_0^2\epsilon_{e+}}P_i^+P_k^+ \\ &+ \sum_{m=e,o}\int_0^{k_t}\frac{q(\rho, k_t)}{k_0^2-\rho^2}Q_{im}^+(\rho)\,Q_{km}^+(\rho)\,d\rho \\ &+ \int_0^{v}\frac{p(\sigma, k_t)}{k_0^2\epsilon_2-\sigma^2}S_i^+(\sigma)\,S_k^+(\sigma)\,d\sigma\end{aligned}$$

$$\begin{aligned}\text{Im}\ \{\mathbf{Z}(k_t)\}_{ik} &= -\sum_{m=e,o}\int_{k_t}^{\infty}\frac{\gamma(\rho, k_t)}{k_0^2-\rho^2}Q_{im}^+(\rho)\,Q_{km}^+(\rho)\,d\rho \\ &+ \frac{q_s(k_t)}{k_0^2\epsilon_{e-}}P_i^-P_k^-\,tg[q_s(k_t)a] \\ &+ \sum_{m=e,o}\int_0^{\infty}\frac{q(\rho, k_t)}{k_0^2-\rho^2}Q_{im}^-(\rho)\,Q_{km}^-(\rho) \\ &\cdot tg[q(\rho, k_t)a]\,d\rho + \int_0^{v}\frac{p(\sigma, k_t)}{k_0^2\epsilon_2-\sigma^2} \\ &\cdot S_i(\sigma)\,S_k(\sigma)\,tg[p(\sigma, k_t)a]\,d\sigma.\end{aligned}$$

$tg\alpha_v(k_t)$ is the eigenvalue of (6), $\boldsymbol{H}_v$ is the eigenvector and $\text{Re}\ \{\mathbf{Z}(k_t)\}$ is a weight matrix. The eigenvector is just the v-th component of the interface field $h_{yv}(y, k_t)$ in the basis (5). For this kind of problem, the following orthogonality relationship on the interface $x = 0$ holds (T denotes transposition):

$$\boldsymbol{H}_v^T \cdot \text{Re}\ \{\mathbf{Z}(k_t)\} \cdot \boldsymbol{H}_\mu = \delta_{v\mu}. \tag{7}$$

The physical interpretation of (7) is that two field distributions pertaining to the same k_t, but corresponding to different indices μ, ν, are also orthogonal in y over the interface at $x = 0$, i.e. they do not exchange power at this discontinuous interface.

In order to actually set up and solve (6) while keeping the matrix size as low as possibe, we must effect a prudent choice of the expansion basis for the field at the interface, that includes all known physical features of the solution. In fact, we use a single function, the 'transition function' [1], [2], a choice that makes this problem scalar. The 'transition function' consists of the distribution of the component h_{yt} of the guided mode of a slab of intermediate height, that maximizes the coupling integrals between the slabs to the left and to the right of the transverse discontinuity and the intermediate slab itself. With this choice $N = 1$ in (5), and either (4) or (6) becomes the scalar equation below:

$$\begin{aligned}tg\alpha(k_t) = \Bigg\{&-\sum_{m=e,o}\int_{k_t}^{\infty}\frac{\gamma(\rho, k_t)}{k_0^2-\rho^2}[Q_m^+(\rho)]^2\,d\rho \\ &+ \frac{q_s(k_t)}{k_0^2\epsilon_{e-}}[P^-]^2tg[q_s(k_t)a] \\ &+ \sum_{m=e,o}\int_0^{\infty}\frac{q(\rho, k_t)}{k_0^2-\rho^2} \\ &\cdot [Q_m^-(\rho)]^2tg[q(\rho, k_t)a]\,d\rho \\ &+ \int_0^{v}\frac{p(\sigma, k_t)}{k_0^2\epsilon_2-\sigma^2}[S^-(\sigma)]^2tg[p(\sigma, k_t)a]\,d\sigma\Bigg\} \\ &\cdot\Bigg\{\frac{k_x(k_t)}{k_0^2\epsilon_{e+}}[P^+]^2 + \sum_{m=e,o}\int_0^{k_t}\frac{q(\rho, k_t)}{k_0^2-\rho^2} \\ &\cdot [Q_m^+(\rho)]^2\,d\rho + \int_0^{v}\frac{p(\sigma, k_t)}{k_0^2\epsilon_2-\sigma^2}[S^+(\sigma)]^2\,d\sigma\Bigg\}^{-1}.\end{aligned} \tag{8}$$

Although (8) is now a scalar expression, its pointwise numerical evaluation is time-consuming in practice and a simpler expression would be desirable. One such is obtained by observing in (8) that the behavior of $tg\alpha(k_t)$ is dominated by its poles, arising from the factor $tg[q_s(k_t)a]$ in the second term. Considering the asymptotic behaviour around these poles, one recovers a simple approximate expression, valid for not too large a rib height t, namely,

$$tg\alpha(k_t) = \left(\frac{P^-}{P^+}\right)^2 \frac{\epsilon_{e+}}{\epsilon_{e-}} \frac{q_s(k_t)}{k_x(k_t)} tg[q_s(k_t)a]. \qquad (9)$$

In order to assess the validity of this approximation, we compute $tg\alpha(k_t)$ for two significant cases of rib waveguide with $n_1 = 3.44$, $n_2 = 3.35$, $\lambda = 1.15$ μm, $D = 1$ μm, $a = 1.5$ μm, $d = 0.5$ μm and 0.9 μm, respectively.

Outer slab thicknesses $d = 0.5$ μm and 0.9 μm represent the situations of slabs guides near and beyond cutoff respectively. The results for $tg\alpha(k_t)$ versus k_t/k_0 predicted from equations (8) (continuous line) and (9) (dashed line) are plotted in Fig. 2 and Fig. 3 for $d = 0.5$ μm and $d = 0.9$ μm respectively. From these figures, we notice that the difference between the two curves is very small, even for large steps, as long as the outer slab supports surface modes. Moreover, in the case of Fig. 3, the two curves can be considered coincident. However, where the outer slab is below cutoff, approximation (9) does not hold and (8) must be used instead, taking care of suppressing the term P^+ that corresponds to a guided mode of the outer slab, now nonpropagating.

Once the eigenvalue $\alpha(k_t)$ is recovered, all field components of the continuous modes are obtainable from the expression (2a), (2b) of the hertzian potentials.

Finally, in Appendix I is shown that for the continuum the following orthonormality condition holds:

$$\iint_S \boldsymbol{E}_\nu(x, y, k_t) \times \boldsymbol{H}_\mu(x, y, k_t') \cdot z \, ds = \delta_{\mu\nu} \, \delta(k_t - k_t'). \qquad (10)$$

(10) implies in (2a), (2b) the following normalization coefficient:

$$\sqrt{\frac{2k_t}{\pi\omega\mu\beta(k_t)}} \cos \alpha_\nu(k_t).$$

Extension to the odd case (magnetic wall in $x = -a$) is obvious.

Analogous developments are applied to the substrate continuous modes in terms of the independent continuous variable σ_t. The complete expression of this kind of modes are reported in Appendix II. Using again the 'transition function', we can obtain a simplified expression of the $tg\delta(\sigma_t)$, valid for not too large ribs:

$$tg\delta(\sigma_t) = \left(\frac{P^-}{P^+}\right)^2 \frac{\epsilon_{e+}}{\epsilon_{e-}} \frac{k_s(\sigma_t)}{\sigma_x(\sigma_t)} tg[k_s(\sigma_t)a]. \qquad (11)$$

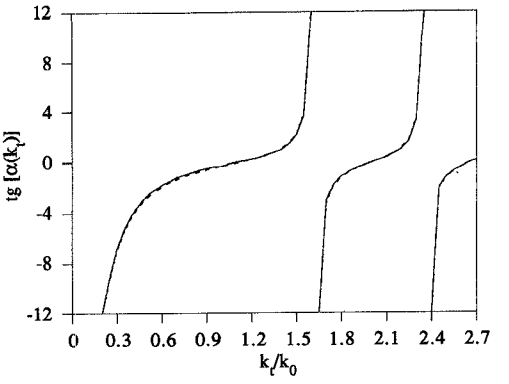

Fig. 2. Values of $tg\alpha(k_t)$ versus k_t/k_0 predicted form (8) (continuous line) and (9) (dashed line) for the following parameters: $n_1 = 3.44$, $n_2 = 3.35$, $\lambda = 1.15$ μm, $D = 1$ μm, $a = 1.5$ μm and $d = 0.5$ μm.

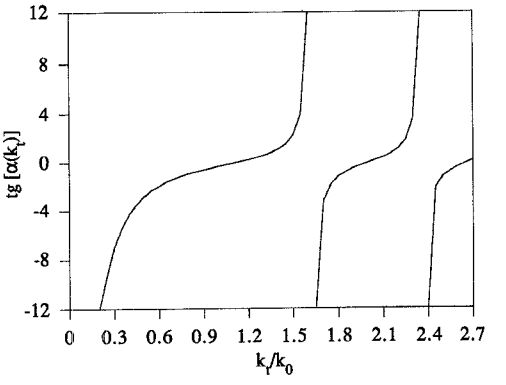

Fig. 3. Values of $tg\alpha(k_t)$ versus k_t/k_0 predicted form (8) (continuous line) and (9) (dashed line) for the following parameters: $n_1 = 3.44$, $n_2 = 3.35$, $\lambda = 1.15$ μm, $D = 1$ μm, $a = 1.5$ μm and $d = 0.9$ μm.

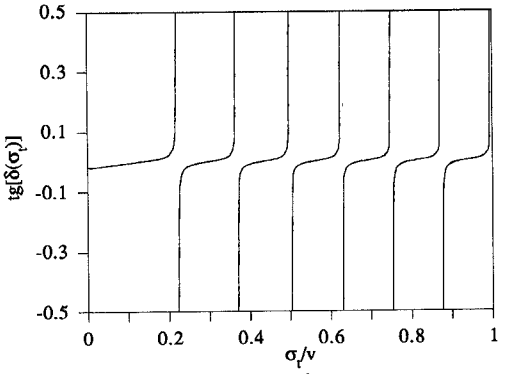

Fig. 4. Values of $tg\sigma(\sigma_t)$ versus σ_t/v predicted from (11) (continuous line) and (A2.3) (dashed line) for the following parameters: $n_1 = 3.44$, $n_2 = 3.35$, $\lambda = 1.15$ μm, $D = 1$ μm, $a = 1.5$ μm and $d = 0.5$ μm.

As in the previous case, we can compare the behaviour of $tg\delta(\sigma_t)$ obtained by (11) with the complete expression reported in Appendix II (A2.3). We have considered the same cases of the $tg\alpha(k_t)$, i.e.: $n_1 = 3.44$, $n_2 = 3.35$, $\lambda = 1.15$ μm, $D = 1$ μm, $a = 1.5$ μm, $d = 0.5$ μm and 0.9 μm. We notice that the complete expression (A2.3) is well approximated by (11), as shown in Figs. 4 and 5, where the two curves are practically coincident.

Moreover, we notice that $tg\delta(\sigma_t)$ evaluated at $\sigma_t = v$ is exactly equal to the value of $tg\alpha(k_t)$ at $k_t = 0$. Thus, we

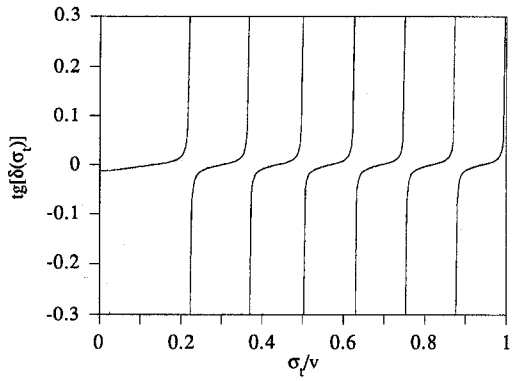

Fig. 5. Values of $tg\delta(\sigma_t)$ versus σ_t/v predicted from (11) (continuous line) and (A2.3) (dashed line) for the following parameters: $n_1 = 3.44$, $n_2 = 3.35$, $\lambda = 1.15$ μm, $D = 1$ μm, $a = 1.5$ μm and $d = 0.9$ μm.

can assert that the substrate continuous modes are the 'continuation' of the air continuous modes.

Step Discontinuities in Rib Guide

Knowledge of the continuous spectrum is now applied to various examples of step discontinuities.

Step discontinuities were examined in the literature [4] but the presence of a rib guide continuum was never introduced. The continuum, in fact, plays the same role as that of higher order modes in close guide, that are excited by a step discontinuity.

E-Plane Step

The first case under consideration is the discontinuity in the E-plane of a LSE-polarized rib guide due to a change of rib width occurring at $z = 0$, as shown in Fig. 6.

By standard techniques [13], we recover the integral equation for the discontinuity in terms of the transverse magnetic field distribution H_y at the step:

$$\frac{1+R}{1-R}A^- e_x^-(x,y) - \int_0^\infty A^-(k_t)\, e_x^-(x,y,k_t)\, dk_t + \int_0^v A^-(\sigma_t)\, e_x^-(x,y,\sigma_t)\, d\sigma_t = A^+ e_x^+(x,y) + \int_0^\infty A^+(k_t)\, e_x^+(x,y,k_t)\, dk_t + \int_0^v A^+(\sigma_t)\, e_x^+(x,y,\sigma_t)\, d\sigma_t \quad (12)$$

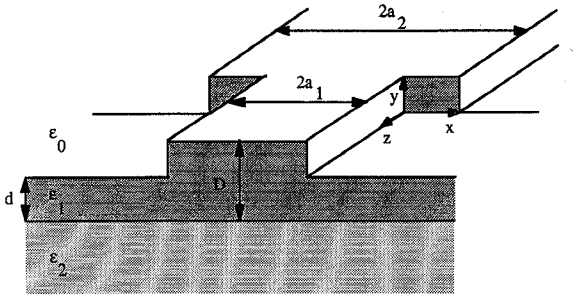

Fig. 6. Change in rib width between two rib waveguides.

with

$$A^- = \langle\langle H_y, e_x^-(x,y)\rangle\rangle$$
$$A^+ = \langle\langle H_y, e_x^+(x,y)\rangle\rangle$$
$$A^-(k_t) = \langle\langle H_y, e_x^-(x,y,k_t)\rangle\rangle$$
$$A^+(k_t) = \langle\langle H_y, e_x^+(x,y,k_t)\rangle\rangle$$
$$A^-(\sigma_t) = \langle\langle H_y, e_x^-(x,y,\sigma_t)\rangle\rangle$$
$$A^+(\sigma_t) = \langle\langle H_y, e_x^+(x,y,\sigma_t)\rangle\rangle$$

where $\langle\langle\ \rangle\rangle$ stands for the integration over the cross-section, $e_x^-(x,y)$, $e_x^-(x,y,k_t)$, $e_x^-(x,y,\sigma_t)$, $e_x^+(x,y)$, $e_x^+(x,y,k_t)$, $e_x^+(x,y,\sigma_t)$, denote the x-components of the electric field of the bound modes and of the continua, to the left and to the right of the discontinuity, respectively, and the normalizations (10) and (A2.4) hold.

Again, using the 'transition function' as a single term expansion reduces the above equation (12) to a scalar one: we take as H_y the transverse distribution of the bound mode of an ideal rib guide of width intermediate between a_1 and a_2, so as to ensure maximum conservation of power at the step discontinuity. By multiplying (12) by H_y and integrating in the transverse section, a relatively simple expression of the reflection coefficient is obtained:

$$R = \frac{A^{+2} - A^{-2} + \int_0^\infty [A^{-2}(k_t) + A^{+2}(k_t)]\, dk_t + \int_0^v [A^{-2}(\sigma_t) + A^{+2}(\sigma_t)]\, d\sigma_t}{A^{-2} + A^{+2} + \int_0^\infty [A^{-2}(k_t) + A^{+2}(k_t)]\, dk_t + \int_0^v [A^{-2}(\sigma_t) + A^{+2}(\sigma_t)]\, d\sigma_t}. \quad (13)$$

Now, the above overlapping integrals can be evaluated analytically. The results obtained for modulus and phase of the reflection coefficient at the step discontinuity of Fig. 6 are shown in Fig. 7, assuming the following parameter values: $n_1 = 3.44$, $n_2 = 3.40$, $\lambda = 1.15$ μm, $2a_2 = 3$ μm, $d = 0.6$ μm and $D = 1.0$ μm.

In the same manner, we have examined the abruptly terminated rib waveguide shown in Fig. 8. In particular, in Fig. 8(a) just the rib is terminated, in Fig. 8(b) the guide and the surrounding slab are terminated and, finally, in Fig. 8(c) the whole guide is terminated. Correspondingly, the region $z > 0$ is represented by the spectrum of an asymmetrical slab waveguide of thickness d for the case of Fig. 8(a), by the spectrum of an air-sub-

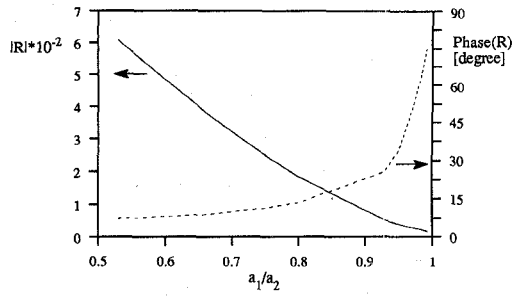

Fig. 7. Modulus and phase of the reflection coefficient versus w_1/w_2 for the case of Fig. 6 with the following parameters: $\epsilon_1 = 3.44$, $\epsilon_2 = 3.40$, $\lambda = 1.15$ μm, $2a_2 = 3$ μm, $d = 0.6$ μm and $D = 1.0$ μm.

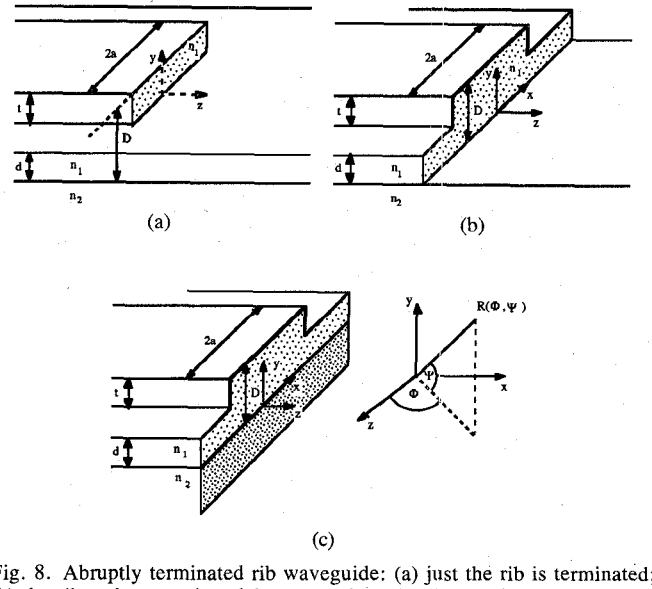

Fig. 8. Abruptly terminated rib waveguide: (a) just the rib is terminated; (b) the rib and supporting slab are terminated; (c) the whole guide is terminated.

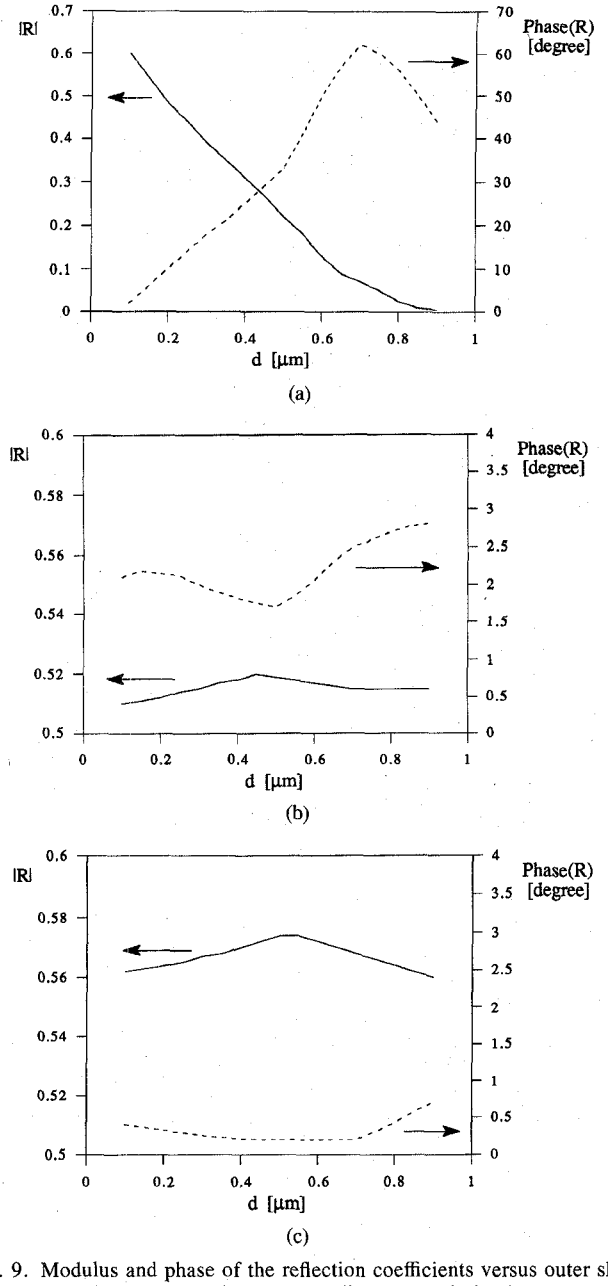

Fig. 9. Modulus and phase of the reflection coefficients versus outer slab thickness d for the corresponding cases of Fig. 8.

strate space for the case of Fig. 8(b) and by the spectrum of the air space in case of Fig. 8(c). Now, for case of Fig. 8(a) we use as 'transition function' the bound mode of a rib waveguide whose height $\bar{d}$ is intermediate between those of the guide 'D' and the slab 'd' to the left and to the right of the step respectively. Again $\bar{d}$ is chosen so as to ensure maximum conservation of power.

In the case where no guidance is present in region $z \geq 0$, i.e. for cases of Fig. 8(b) and 8(c), the above criterion breaks down. For these cases, we choose as 'transition function' the bound mode of the rib waveguide whose height is the same as the height of the 'transition slab', as defined in the previous section.

Although this choice is somewhat arbitrary, its use is justified by the insensivity of the results to slight variations of the variational trial function.

The reflection coefficients for the cases of Fig. 8 are shown in Fig. 9. In the case of Fig. 9(a) where only the rib is terminated at $z = 0$, the reflection coefficient decreases as d increases. This is to be expected, since, as d increases, the rib waveguide approaches the asymmetrical slab guide at $z \geq 0$ and most of the incident wave from the rib guide will transmit through to the asymmetrical slab guide for $z \geq 0$. As the confinement increases, i.e., d decreases, the reflection coefficient of configuration of Fig. 8(a) approaches that of Fig. 8(b). This is so because, as d decreases, the slab at $z \geq 0$ will not support surface waves and there is no guiding.

The reflection coefficient of the configuration of Fig. 8(c) where the guide is terminated by the air half space is slightly higher than those of Fig. 8(b) or Fig. 8(a) with a slab below cutoff. This suggests that some of incident wave leaks through the substrate. However, the difference in the reflection coefficients of the two different terminations is not large.

Finally, the forward and backscattered radiation patterns of the far field for the configuration of Fig. 8(c), calculated by means of saddle point integration, are shown

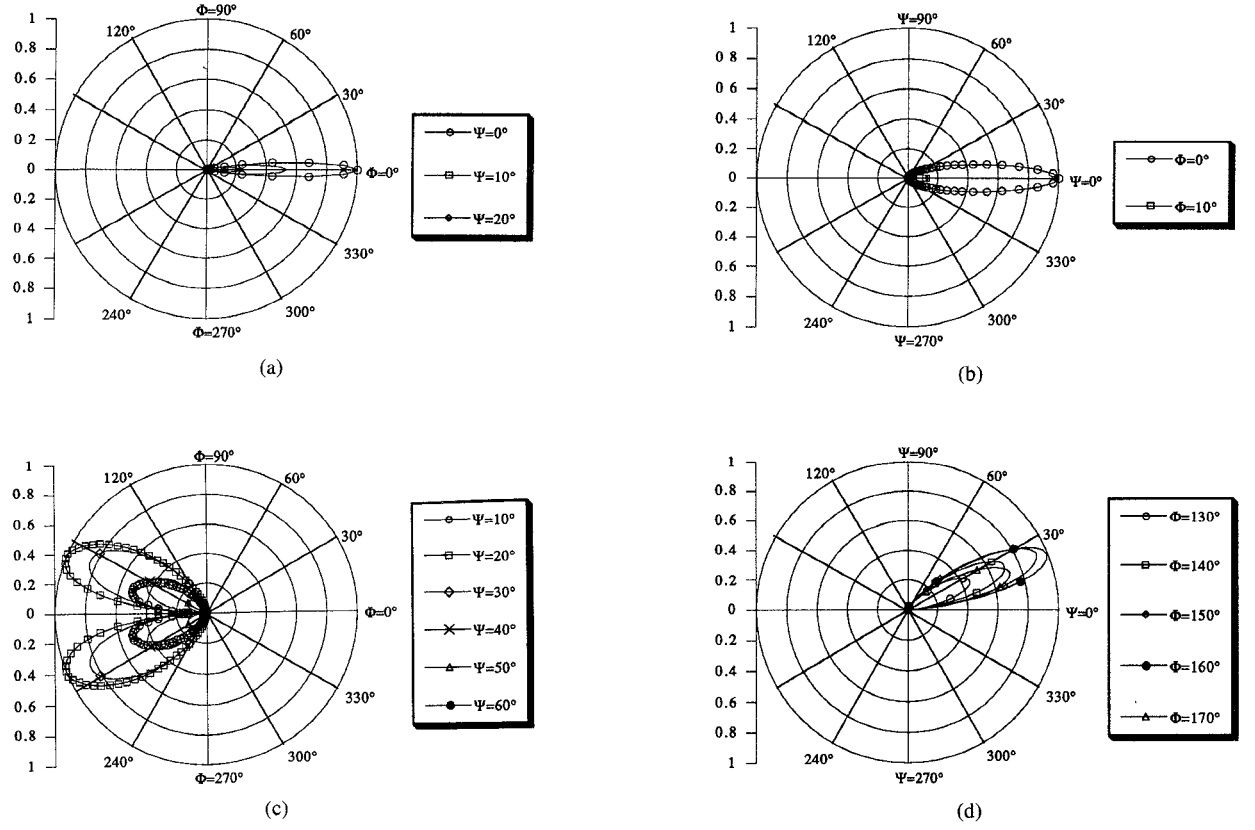

Fig. 10. Forward and backscattered radiation patterns of the far field for the configuration of Fig. 8(c): (a) Φ-plane and (b) Ψ-plane for forward radiation; (c) Φ-plane and (d) Ψ-plane for backward radiation.

in Fig. 10, where the curves with negligible value have not been reported, for the sake of simplicity.

Fig. 10(a)–(b) show the forward radiation pattern in the azimuthal and transverse directions (see Fig. 8(c)). We notice a narrow lobe in Φ as well as in Ψ, at about $\Phi \approx 0°$, $\Psi \approx 0°$. Fig. 10(c)–(d) show the backward radiation pattern. In the Φ-plane we notice that the maximum radiation occurs at about $\Phi \approx 160°$, $\Psi \approx 20°$. Obviously, this radiation is symmetrical with respect to the plane $\Phi = \pi$.

In the Ψ-plane, the maximum is at about $\Psi \approx 25°$, $\Phi \approx 160°$. In the latter radiation pattern, the air region is represented by $0° \leq \Psi \leq 90°$, the substrate region is represented by $270° \leq \Psi \leq 360°$. Note, however, that the radiation patterns are normalized to its maximum value and the backscattered radiation in this problem is about three order of magnitude less than the forward radiation. We note the presence of backscattered radiation over a wide range of angles, not unlike the case of a step discontinuity in slab guide [13].

This last result would be particularly difficult to obtain without a knowledge of the rib guide radiation modes.

Conclusion

We have derived the continuous spectrum of the rib waveguide by a method that ensures orthonormality and completeness of the spectrum. We obtain a relatively simple approximation of this continuum for most cases of common interest. Finally, we used the complete spectrum of the rib waveguide to examine various cases of step discontinuities, including, for the first time, radiative effects.

Appendix I

Setting $\Delta(\rho) = k_0^2 - \rho^2$, $\Delta(\sigma) = k_0^2\epsilon_2 - \sigma^2$ and dropping the k_t-dependence when not necessary, integral (10) can be divided into two parts: one for the inner region (I_1) and one for the outer region (I_2).

We have

$$I_1 = \int_{-a}^{0}\int_{-\infty}^{\infty} E_{xv}(x, y, k_t)\, H_{y\mu}(x, y, k_t')\, dx\, dy$$

$$= \frac{2}{\pi}\cos\alpha_v(k_t)\cos\alpha_\mu'(k_t)\sqrt{\frac{k_t k_t'\beta}{\beta'}}$$

$$\cdot\left\{\frac{P_v^- P_\mu^-}{k_0^2\epsilon_{e-}}\frac{q_s tg(q_s a) - q_s' tg(q_s' a)}{q_s^2 - q_s'^2}\right.$$

$$+ \sum_{m=e,o}\int_0^\infty \frac{Q_{vm}^- Q_{\mu m}^-}{\Delta(\rho)}\frac{qtg(qa) - q' tg(q' a)}{q^2 - q'^2}\, d\rho$$

$$\left. + \int_0^v \frac{S_v^- S_\mu^-}{\Delta(\sigma)}\frac{ptg(pa) - p' tg(p' a)}{p^2 - p'^2}\, d\sigma\right\}$$

If $k_t \leq k_t'$:

$$I_2 = \int_0^\infty \int_{-\infty}^\infty E_{xv}(x, y, k_t)\, H_{y\mu}(x, y, k_t')\, dx\, dy$$

$$= \sqrt{\frac{k_t k_t' \beta}{\beta'}} \left\{ I_{21}\, \delta(k_t - k_t') + \frac{2}{\pi} \cdot \frac{\cos \alpha_v(k_t) \cos \alpha_\mu'(k_t)}{k_t^2 - k_t'^2} I_{22} \right\}$$

where

$$I_{21} = \frac{k_x}{k_t} \frac{P_v^+ P_\mu^+}{k_0^2 \epsilon_{e+}} + \sum_{m=e,o} \int_0^\infty \frac{q}{k_t \Delta(\rho)} Q_{vm}^+ Q_{\mu m}^+ \, d\rho + \int_0^v \frac{p}{k_t \Delta(\sigma)} S_v^+ S_\mu^+ \, d\sigma$$

$$I_{22} = P_v^+ P_\mu^+ \frac{-k_x tg\alpha_v + k_x' tg\alpha_v'}{k_0^2 \epsilon_{e+}} - \sum_{m=e,o} \int_0^{k_t} \frac{q tg\alpha_v - k_x' tg\alpha_v'}{\Delta(\rho)} Q_{vm}^+ Q_{\mu m}^+ \, d\rho - \sum_{m=e,o} \int_{k_t}^{k_t'} \frac{\gamma - k_x' tg\alpha_v'}{\Delta(\rho)} Q_{vm}^+ Q_{\mu m}^+ \, d\rho - \sum_{m=e,o} \int_{k_t'}^\infty \frac{\gamma - \gamma'}{\Delta(\sigma)} Q_{vm}^+ Q_{\mu m}^+ \, d\rho - \int_0^v \frac{p tg\alpha_v - p' tg\alpha_v'}{\Delta(\sigma)} S_v^+ S_\mu^+ \, d\sigma.$$

Taking into account that $q_s^2 - q_s'^2 = q^2 - q'^2 = p^2 - p'^2 = k_t^2 - k_t'^2$, and expanding h_{yv} as in (5), by the definition (6) of $tg\alpha_v(k_t)$, the sum of I_1 and of the second term of I_2 gives zero. Thus, by (7), the remaining term yields

$$\iint_S \boldsymbol{E}_v(x, y, k_t) \times \boldsymbol{H}_\mu(x, y, k_t') \cdot z \, ds = \delta(k_t - k_t') \boldsymbol{H}_v^T \operatorname{Re}\{\tilde{\boldsymbol{Z}}(k_t)\} \boldsymbol{H}_\mu = \delta(k_t - k_t')\, \delta_{v\mu}.$$

Appendix II

The complete expression valid for substrate continuous modes is

$$\Pi_v^h(x, y, \sigma_t) = \frac{P_v^-}{k_0^2 \epsilon_{e-}} \phi_s(y) \frac{\cos[k_s(\sigma_t)(x + a)]}{\cos[k_s(\sigma_t) a]} + \sum_{m=e,o} \int_0^\infty \frac{Q_{vm}^-(\rho)}{k_0^2 - \rho^2} \phi_m(\rho, y) \cdot \frac{ch[k(\rho, \sigma_t)(x + a)]}{ch[k(\rho, \sigma_t) a]} \, d\rho + \int_0^{\sigma_t} \frac{S_v^-(\sigma)}{k_0^2 \epsilon_2 - \sigma^2} \phi_{sb}(\sigma, y) \cdot \frac{\cos[\xi(\sigma, \sigma_t)(x + a)]}{\cos[\xi(\sigma, \sigma_t) a]} \, d\sigma + \int_{\sigma_t}^v \frac{S_v^-(\sigma)}{k_0^2 \epsilon_2 - \sigma^2} \phi_{sb}(\sigma, y) \cdot \frac{ch[\xi(\sigma, \sigma_t)(x + a)]}{ch[\xi(\sigma, \sigma_t) a]} \, d\sigma \qquad -a \leq x \leq 0 \qquad \text{(A2.1)}$$

$$\Pi_v^h(x, y, \sigma_t) = \frac{P_v^+}{k_0^2 \epsilon_{e+}} \psi_s(y) \frac{\cos[\sigma_x(\sigma_t) x + \delta_v(\sigma_t)]}{\cos \delta_v(\sigma_t)} + \sum_{m=e,o} \int_0^\infty \frac{Q_{vm}^+(\rho)}{k_0^2 - \rho^2} \psi_m(\rho, y) \cdot e^{-k(\rho, \sigma_t) x} \, d\rho + \int_0^{\sigma_t} \frac{S_v^+(\sigma)}{k_0^2 \epsilon_2 - \sigma^2} \psi_{sb}(\sigma, y) \cdot \frac{\cos[\xi(\sigma, \sigma_t) x + \delta_v(\sigma_t)]}{\cos \delta_v(\sigma_t)} \, d\sigma + \int_{\sigma_t}^v \frac{S_v^+(\sigma)}{k_0^2 \epsilon_2 - \sigma^2} \psi_{sb}(\sigma, y) e^{-\zeta(\sigma, \sigma_t) x} \, d\sigma \qquad x \geq 0 \qquad \text{(A2.2)}$$

where

$$\sigma_x(\sigma_t) = \sqrt{\sigma_t^2 + k_0^2(\epsilon_{e+} - \epsilon_2)} \qquad k_s(\sigma_t) = \sqrt{\sigma_t^2 + k_0^2(\epsilon_{e-} - \epsilon_2)}$$

$$\xi(\sigma, \sigma_t) = \sqrt{\sigma_t^2 - \sigma^2} \qquad k(\rho, \sigma_t) = \sqrt{\rho^2 - \sigma_t^2 + v^2}$$

$$\zeta(\sigma, \sigma_t) = \sqrt{\sigma^2 - \sigma_t^2} \qquad v = k_0 \sqrt{\epsilon_2 - 1}.$$

$$P_v^- = \int_{-\infty}^\infty h_{yv}(y, \sigma_t)\, \phi_s(y)\, dy \equiv \langle h_{yv}(y, \sigma_t), \phi_s(y) \rangle \qquad P_v^+ = \langle h_{yv}(y, \sigma_t), \psi_s(y) \rangle$$

$$Q_{vm}^-(\rho) = \langle h_{yv}(y, \sigma_t), \phi_m(\rho, y) \rangle \qquad Q_{vm}^+(\rho) = \langle h_{yv}(y, \sigma_t), \psi_m(\rho, y) \rangle$$

$$S_v^-(\sigma) = \langle h_{yv}(y, \sigma_t), \phi_{sb}(\sigma, y) \rangle \qquad S_v^+(\sigma) = \langle h_{yv}(y, \sigma_t), \psi_{sb}(\sigma, y) \rangle.$$

With analogous development to that of the air continuous modes, introducing the 'transition function', we obtain:

$$tg\delta_\nu(\sigma_t)\left\{\frac{\sigma_x(\sigma_t)}{k_0^2\epsilon_{e+}}[P^+]^2+\int_0^{\sigma_t}\frac{\xi(\sigma,\sigma_t)}{k_0^2\epsilon_2-\sigma^2}S^+(\sigma)]^2\,d\sigma\right\}$$

$$=\frac{k_s(\sigma_t)}{k_0^2\epsilon_{e-}}[P^-]^2tg[k_s(\sigma_t)a]$$

$$-\sum_{m=e,o}\int_0^\infty\frac{k(\rho,\sigma_t)}{k_0^2-\rho^2}[Q_m^+(\rho)]^2\,d\rho$$

$$-\sum_{m=e,o}\int_0^\infty\frac{k(\rho,\sigma_t)}{k_0^2-\rho^2}[Q_m^-(\rho)]^2tgh[k(\rho,\sigma_t)a]\,d\rho$$

$$-\int_{\sigma_t}^{v}\frac{\zeta(\sigma,\sigma_t)}{k_0^2\epsilon_2-\sigma^2}[S^+(\sigma)]^2\,d\sigma$$

$$+\int_0^{\sigma_t}\frac{\xi(\sigma,\sigma_t)}{k_0^2\epsilon_2-\sigma^2}[S^-(\sigma)]^2tg[\xi(\sigma,\sigma_t)a]\,d\sigma$$

$$-\int_{\sigma_t}^{v}\frac{\zeta(\sigma,\sigma_t)}{k_0^2\epsilon_2-\sigma^2}[S^-(\sigma)]^2tgh[\zeta(\sigma,\sigma_t)a]\,d\sigma. \tag{A2.3}$$

Moreover, the following orthogonality relationships hold:

$$\iint_S \boldsymbol{E}_\nu(x,y,\sigma_t)\times\boldsymbol{H}_\mu(x,y,\sigma_t')\cdot z\,ds$$

$$=\delta_{\mu\nu}\,\delta(\sigma_t-\sigma_t')$$

$$\iint_S \boldsymbol{E}_\nu(x,y,k_t)\times\boldsymbol{H}_\mu(x,y,\sigma_t)\cdot z\,ds$$

$$=\iint_S \boldsymbol{E}_\nu(x,y,\sigma_t)\times\boldsymbol{H}_\mu(x,y,k_t)\cdot z\,ds=0 \tag{A2.4}$$

(A2.4) introduces in (A2.1), (A2.2) the following normalization coefficient:

$$\sqrt{\frac{2\sigma_t}{\pi\omega\mu\beta(\sigma_t)}}\cos\delta_\nu(\sigma_t). \tag{A2.5}$$

References

[1] M. Koshiba and M. Suzuki, "Vectorial wave analysis of dielectric waveguides for optical-integrated circuits using equivalent network approach," *J. Lightwave Technol.*, vol. LT-4, pp. 656–664, June 1986.

[2] T. Rozzi, G. Cerri, M. N. Husain, and L. Zappelli, "Strongly coupled dielectric rib waveguides, use of the transition function and of edge discontinuities," *Proc. 19th European Microwave Conf.*, Sept. 1989, pp. 1147–1154.

[3] ——, "Variational analysis of the dielectric rib waveguide using the concept of transition function and including edge singularities," *IEEE Trans. Microwave Theory Tech.*, vol. 39, no. 2, pp. 247–257, Feb. 1991.

[4] B. M. A. Rahman, J. B. Davies, "Analysis of optical waveguides and some discontinuity problems," *Proc. Inst. Elec. Eng.*, vol. 135, pt. J, no. 5, Oct. 1988.

[5] T. Rozzi, G. Cerri, F. Chiaraluce, R. De Leo, and R. F. Ormondroyd, "Finite curvature and corrugations in dielectric ridge waveguides," *IEEE Trans. Microwave Theory Tech.*, vol. 36, no. 1, pp. 68–79, Jan. 1991.

[6] J. S. Gu, P. A. Besse, and H. Melchior, "Novel method for analysis of curved optical rib waveguides," *Electron. Lett.*, vol. 25, no. 4, pp. 278–280, Feb. 1989.

[7] ——, "Method of lines for the analysis of the propagation characteristics of curved optical rib waveguides," *IEEE J. Quantum Electron.*, vol. 27, no. 3, pp. 531–537, Mar. 1991.

[8] Y. Chung and N. Dagli, "Explicit finite difference beam propagation method: application to semiconductor rib waveguide Y-junction anaysis," *Electron. Lett.*, vol. 26, no. 11, pp. 711–713, May 1990.

[9] T. Rozzi and J. S. Kot, "The complete spectrum of image line," *IEEE Trans. Microwave Theory Tech.*, vol. 37, no. 5, pp. 868–874, May 1989.

[10] S. T. Peng and A. A. Oliner, "Guidance and leakage properties of a class of open dielectric waveguides: Part I—Mathematical formulation," *IEEE Trans. Microwave Theory Tech.*, vol. MTT-29, pp. 843–855, Sept. 1981.

[11] A. A. Oliner, S. T. Peng, T. I. Hsu, and A. Sanchez, "Guidance and leakage properties of a class of open dielectric waveguides: Part II—new physical effects," *IEEE Trans. Microwave Theory Tech.*, vol. MTT-29, pp. 856–869, Sept. 1981.

[12] C. Yeung, T. Rozzi, and G. Cerri, "Crosspolarization coupling in curved dielectric rib waveguides," *Proc. Inst. Elec. Eng.*, vol. 135, pt. J, no. 3, pp. 281–284, June 1988.

[13] T. Rozzi, "Rigorous analysis of the step discontinuity in a planar dielectric waveguide," *IEEE Trans. Microwave Theory Tech.*, vol. MTT-26, pp. 738–746, Oct. 1978.

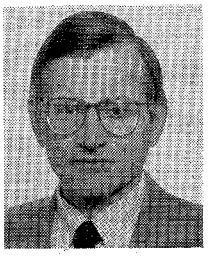

Tullio Rozzi (M'66–SM'74–F'90) obtained the degree of 'Dottore' in physics from the University of Pisa in 1965, and the Ph.D. degree in electronic engineering from Leeds University in 1968. In June 1987 he received the degree of D.Sc. from the University of Bath, Bath, U.K.

From 1968 to 1978 he was a Research Scientist at the Philips Research Laboratories, Eindhoven, the Netherlands, having spent one year, 1975, at the Antenna Laboratory, University of Illinois, Urbana. In 1975 he was awarded the Microwave Prize by the IEEE Microwave Theory and Technique Society.

In 1978 he was appointed to the Chair of Electrical Engineering at the University of Liverpool and was subsequently appointed to the Chair of Electronics and Head of the Electronics Group at the University of Bath, in 1981. From 1983 to 1986 he held the additional position of Head of the School of Electrical Engineering at Bath. Since 1988 he has been Professor of Antennas in the Department of Electronics and Control, University of Ancona, Italy, while remaining a visiting professor at Bath University. Dr. Rozzi is also a Fellow of the IEE (U.K.).

Leonardo Zappelli was born in Rome in 1962. He received the "Doctor" degree in electronic engineering in 1987 and the Ph.D. degree in 1992 from the University of Ancona, Italy.

Since 1988, he has been with the Department of Electronics and Automatics at the University of Ancona, Italy, as a researcher assistant. His area of interest are rib waveguides and nonlinear guides for integrated optics and the characterization of TEM cell for e.m. compatibility.

M. N. Husain, photograph and biography not available at the time of publication.